PROCEEDINGS OF SPIE

Photonic crystal nanofiber air-mode cavity with high Q-factor and high sensitivity for refractive index sensing

Ma, Xiaoxue, Chen, Xin, Nie, Hongrui, Yang, Daquan

SPIE.

Photonic crystal nanofiber air-mode cavity with high Q-factor and high sensitivity for refractive index sensing

Xiaoxue Ma[a] , Xin Chen[b], Hongrui Nie[a], Daquan Yang[b*]
[a]International School, Beijing University of Posts and Telecommunications, Beijing 100876, China
[b]State Key Laboratory of Information Photonics and Optical Communications, School of Information and Communication Engineering, Beijing University of Posts and Telecommunications, Beijing 100876, China
[*]ydq@bupt.edu.cn

ABSTRACT

Recently, due to its superior characteristics and simple manufacture, such as small size, low loss, high sensitivity and convenience to couple, the optical fiber sensor has become one of the most promising sensors. In order to achieve the most effective realization of light propagation by changing the structure of sensors, FOM($S \bullet Q/\lambda_{res}$), which is determined by two significant variables Q-factor and sensitivity, as a trade-off parameter should be optimized to a high value. In typical sensors, a high Q can be achieved by confining the optical field in the high refractive index dielectric region to make an interaction between analytes and evanescent field of the resonant mode. However, the ignored sensitivity is relatively low with a high Q achieved, which means that the resonant wavelength shift changes non-obviously when the refractive index increases. Meanwhile, the sensitivity also leads to a less desirable FOM. Therefore, a gradient structure, which can enhance the performance of sensors by achieving high Q and high sensitivity, has been developed by Kim et al. later. Here, by introducing parabolic-tapered structure, the light field localized overlaps strongly and sufficiently with analytes. And based on a one-dimensional photonic-crystal nanofiber air-mode cavity, a creative optical fiber sensor is proposed by combining good stability and transmission characteristics of fiber and strengths of tapered structure, realizing excellent FOM ~4.7×10^5 with high Q-factors (Q~10^6) and high sensitivities (>700 nm/RIU).

Keywords: optical fiber sensor, phC nanofiber air-mode cavity, parabolic-tapered structure, trade-off, high Q, high sensitivity

1. INTRODUCTION

After the optical fiber as a waveguide medium was demonstrated by Chinese scientists Charles K. Kao in the 1960s, the optical fiber technology has been applied extensively. The general use of optical fiber will be regarded as the media to

connect light and measure instruments. Based on the stability and the transmission characteristics of fiber, the other application - sensors have been researched and promoted in many fields, such as building inspection, biomedical, petrochemical, national defense and security. Especially, the nanofiber sensor is taken seriously due to the trend of miniaturization in different fields and its good performances, such as small size, low loss, high sensitivity and convenient to couple, a photonic crystal air mode cavity we designed as a sensor can both translate light and operate directly, which reduces the complexity of manufacture and increases the sensitivity.

Over the past several years, photonic crystals (PhCs) [1-4] have been proposed to realize optical sensors. In former sensors, the maximum optical field is generally confined in the high refractive index dielectric region to achieve a high Q-factor, but due to the low index cladding position, the detected analytes can only interact with the evanescent field of the resonant mode [5]. Thus, the sensitivity always keeps a low value because of the weak interaction between analytes and light field, and some examples shown [6-9], [12-14]. Lai et al.[10] demonstrated PhC sensors with high Q-factors about~7000; However, the S just achieved ~60 nm/RIU(refractive index unit) and the FOM (S • Q/λ_{res} [11]) was ~300. Quan et al. [12] demonstrated a dielectric-mode photonic crystal cavity with an ultra-high Q ~ 1.2 ×10^5; However, the S calculated was only 83 nm/RIU. In order to improve the sensitivity and avoid drastically reducing the Q value, there was a one-dimensional (1D) photonic crystal (PhC) single nanobeam sensor based on the second air band-edge mode, which enables the light intensity be squeezed into the air area and fully overlap with the analytes to achieve a refractive index sensor, with both high sensitivities and high Q-factors [15-19]. For example, Kim et al. [15] demonstrated a nanobeam optical sensor based on the mode, which achieved a high RI sensitivity and FOM, exceeding 631 nm/RIU and 9.5×10^3, respectively. However,the Q-factor was not ideal, about 23,300. Combining the features of fiber with the parabolic-tapered-hole structure and continuously following the air-mode cavity, the simplest and novel structure was designed to increase the stability and sensitivity, with maintaining the high Q factor. In this work, with the highest Q-factor of ~10^6, RI sensitivity achieved a fairly high value of 709 nm/RIU, which corresponds to a high FOM~4.7×10^5, two orders of magnitude enhanced compared to the previous designs.

2. PHC NANOFIBER AIR-MODE CAVITY DESIGN

In the early explorations, Sejeong Kim conducted a detailed research for Q-factor and sensitivity, aiming to compare the first dielectric band-edge mode with the second air band-edge mode [15]. One of the important experiments showed that when the RI changed from 1.33 to 1.43, the resonant wavelengths of the two modes were increasing. The second air band edge pattern increased by 63.1 nm and RI sensitivity was 632 nm/RIU, which was almost 4 times as much as that for the first media band edge pattern (177 nm/RIU). And Kim also proved that due to the absorption of water, the value of Q-factor was limited and the sensor application did not require an excessively high Q value of 10,000 or higher. Therefore, in comparison, the sensitivity is an issue that is more worthy of attention.

On the basis of that, Figure 1(a) shows the schematic of the 1D PhC nanofiber air-mode cavity described in this work. Here, using fiber as a sensor avoids complex design and it is easy to couple, with its refractive index (RI) n_{fiber}= 1.45. The

light is transmitted from the left of the fiber, monitored at the right. With respect to the red dashed line, the structure is symmetric. While the air-mode cavity guarantees the high sensitivity by overlapping sufficiently between the strongly localized light field and analytes, the tapered-hole structure from large holes at the ends to the small holes in the middle maintains the high Q-factor value. The width of the fiber w = 1180 nm and the periodicity a = 620 nm are constant, remaining unchanged. To create a Gaussian mirror, the minimum hole radius at the center of the cavity r_{y_min} = 195 nm increases to the maximum radius r_{y_max} = 240 nm according to a known formula $r_{y\_i} = r_{y\_min} + (r_{y\_max} - r_{y\_min})(i - 1)^2 / (i_{max} - 1)^2$ (i increases from 1 to i_{max}, $i_{max} = 20$), with the extension to both sides.
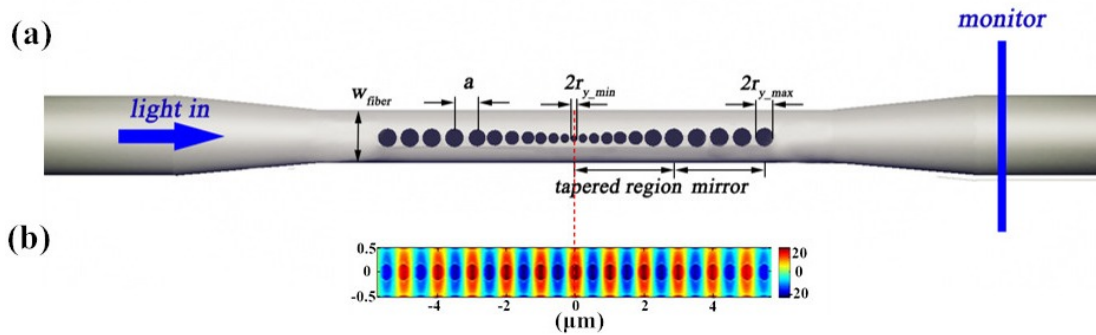

Fig. 1. (a) Schematic of the 1D-PhC nanofiber air-mode cavity sensor. The illustration shows the structure is symmetric about the center of the red dotted line. The periodicity a = 620 nm and the fiber width w=1180 nm keep constant, with tapered hole radius from 195 nm to 240 nm. (b) 3D FDTD simulation of the major field distribution profile (Ey) in the nanofiber air-mode cavity. The number of Gaussian mirror segments i_{max}=20, with an additional 10 mirrors on both ends of the tapering section.

Due to the maximum mirror strength [Fig. 2(b)], the procedure of stimulation involves calculating the mirror strength γ for several different hole radiuses and finding the radius value corresponding to the highest mirror strength among them. The hole radius at the end r_{y_max} = 240 nm is chosen from transverse electric (TE) band-diagram simulations [Fig. 2(a)]. Here, for different radiuses of holes, the mirror strength γ can be calculated by formula $\sqrt{(\omega_2 - \omega_1)^2/(\omega_2 + \omega_1)^2 - (\omega_{res} - \omega_0)^2/\omega_0^2}$, where ω_{res} is the phC single nanofiber air-mode cavity target resonance, and ω_0, ω_1, ω_2 are the mid-gap frequency, dielectric band edge, air band edge of each segment, respectively. Figure 2(a) shows the TE band diagram for the phC single nanofiber air-mode cavity with r_{y_min} = 195 nm (red solid line) and r_{y_max}=240 nm (blue solid line) below the light-line (black dashed line), which is calculated by the 3D finite difference time-domain (FDTD) method (Lumerical Solutions Inc.). The gray shaded region is the photonic bandgap (PBG) for the nanofiber hole radius r_{y_max} = 240 nm and the yellow dot indicates the target resonance frequency (ω_{res}).

In addition, 10 additional mirror segments, keeping the same value of the maximum hole radius r_{y_max}=240nm, are placed at both ends of the Gaussian mirror also contribute to enhancing the Q-factor value. By using the 3D FDTD method, a Q-factor that is obtained at the resonant wavelength of 1365.77 nm almost achieves 10^6. Although the value is not the

highest in the field of photonic crystal sensing research, it is high enough for the reason that the water absorption at telecom wavelengths limits the total Q-factor value of the sensor to 10^4, and in most sensing applications, the water is generally used as the carrier fluid.

The Fig. 1(b), showing the top view of the major field distribution profile (Ey) in the proposed phC single nanofiber air-mode cavity, again verifies that the air mode makes the optical field overlap sufficiently with the analytes within the air region, supporting the fully light–matter interaction. And as it illustrated in the Fig. 1(b), the closer hole is to the middle, the stronger the field strength is. Therefore, the novel 1D-PhC air-mode cavity is proposed in this work as an ideal platform for achieving high-performance RI sensing.
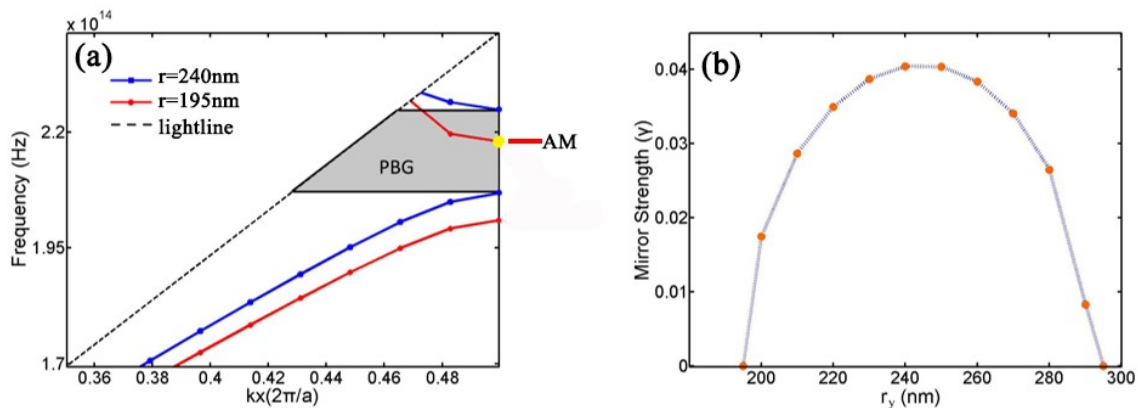

Fig. 2. (a) TE band diagram for the PhC nanofiber air-mode cavity with radiuses r_{y_min} = 195 nm (red solid line) and r_{y_max} = 240 nm (blue solid line). The yellow dot indicates the target resonance frequency. (b) Mirror strengths at different hole radiuses between 195 nm and 300 nm from the 3D band diagram simulation, while keeping the same periodicity a = 620 nm and fiber width w = 1180 nm as in Fig. 1 (a).

3. SIMULATION RESULTS

Figure 3(a) shows the total transmission spectrum. In terms of the simulations, almost 60% transmission is achieved, at the resonant wavelength of 1365.77 nm (n_{air} = 1.0). However, owing to the tapered profile of the air hole radius from small at the center of nanofiber to large on the both sides, the target resonant wavelength is close to the middle of the PBG of the unit cell with the central air hole radius r_{y_min}= 195 nm rather than in the middle as shown in Fig. 2(a). With a smaller hole radius from both ends to the middle, the PBG tends toward a longer wavelength, which results in the target resonant wavelength being close to the band edge of the transmission. The scope of the band-edge modes still agrees well with the band diagram [Fig. 2(a)].

According to Figure 3(b), when the background index changes from RI=1.00 to RI=1.10, the resonant wavelength shift of the fundamental mode is 70.9 nm and by calculation, the RI sensitivity S is up to 709 nm/RIU. Figure 3(c) shows the resonant wavelength shift (red shift) with increasing RI. Although the slope changes slightly with the change in

refractive index, it becomes steeper, which means that the sensitivity may increase continuously on the basis of the tendency of the increasing refractive index. Take the water absorption in the wavelength range of the telecom into account, the Q-factor of the sensor is limited to 10^4 [11] and FOM may remain at up to 4000. Thus, the designed structure possesses a sufficiently high Q ($\sim 10^6$) in many sensing applications and a strongly high sensitivity (709 nm/RIU) to reach an extremely high FOM $\sim 4.7 \times 10^5$, and two orders of magnitude enhanced compared with the previous designs.
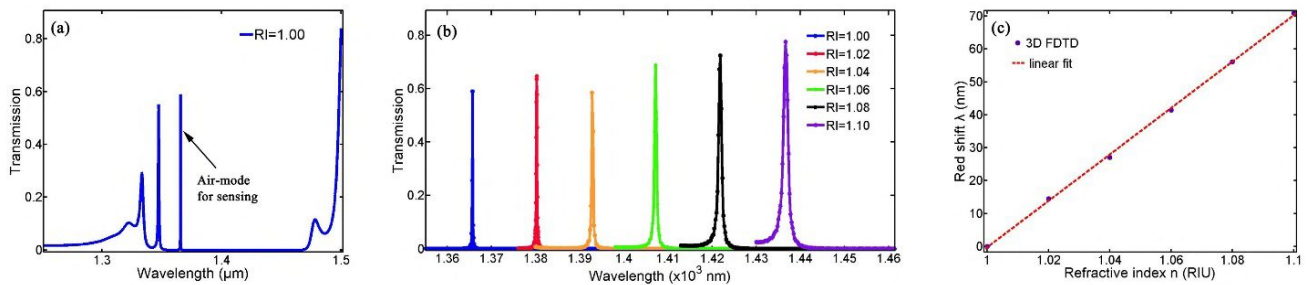

Fig. 3. The optimized structure with N_{taper} = 20 and N_{mirror} = 10 presented by 3D FDTD simulation. (a) Transmission spectrum of the 1D-PhC nanofiber air-mode cavity sensor (RI = 1.00). (b) Transmission spectra variation as the refractive index changes from 1.0 to 1.1. (c) With increasing RI, resonant wavelength shifts regularly.

4. CONCLUSIONS

In this paper, a well trade-off is achieved, while the optimal sensitivities (S = 709 nm/RIU) and Q-factors (Q$\sim 10^6$) at the resonant wavelength of 1365.77 nm for the design are obtained by measurement and constantly optimized, and reaching an unprecedented high FOM$\sim 4.7 \times 10^5$. Breaking the general use of materials for sensor production, the advantages of fiber increases the possibility of coupling and the simplicity of fabrication. Therefore, 1D-PhC simple nanofiber air-mode cavity sensor as a new member in the optical sensors has great space for development and exploitation, moving in the sensitive, compact and intelligent direction. And its other excellent properties, such as anti-electromagnetic and atomic radiation interference performance, high temperature and corrosion resistance of chemical properties, also can be used in other different applications.

REFERENCES

[1] J. Topolancik, P. Bhattacharya, J. Sabarinathan, and P.-C. Yu, "Fluid detection with photonic crystal-based multichannel waveguides," Appl. Phys. Lett. 82, 1143–1145 (2003).

[2] J. Jagerska, H. Zhang, Z. Diao, N. Le Thomas, and R. Houdre, "Refractive index sensing with an air-slot photonic crystal nanocavity," Opt. Lett. 35, 2523–2525 (2010).

[3] M. G. Scullion, A. Di Falco, and T. F. Krauss, "Slotted photonic crystal cavities with integrated microfluidics for biosensing applications," Biosens. Bioelectron. 27, 101–105 (2011).

[4] A. Di Falco, L. O'Faolain, and T. F. Krauss, "Chemical sensing in slotted photonic crystal heterostructure cavities," Appl. Phys. Lett. 94, 063503 (2009).

[5] M. Notomi, "Manipulating light with strongly modulated photonic crystals," Rep. Prog. Phys. 73, 096501 (2010).

[6] X. Zhang, G. Zhou, P. Shi, H. Du, T. Lin, J. Teng, and F. S. Chau, "Onchip integrated optofluidic complex refractive index sensing using silicon photonic crystal nanobeam cavities," Opt. Lett. 41, 1197–1200 (2016).

[7] H. Clevenson, P. Desjardins, X. Gan, and D. Englund, "High sensitivity gas sensor based on high-Q suspended polymer photonic crystal nanocavity," Appl. Phys. Lett. 104, 241108 (2014).

[8] D. Yang, C. Wang, and Y. Jin, "Silicon On-Chip One-Dimensional Photonic Crystal Nanobeam Bandgap Filter Integrated With Nanobeam Cavity for Accurate Refractive Index Sensing," IEEE Photon. J., vol. 8, no. 2, Apr. 2016, Art. no. 4500608.

[9] Q. Quan, F. Vollmer, I. B. Burgess, P. B. Deotare, I. W. Frank, K. Y. Tang, and M. Loncar, "Ultrasensitive on-chip photonic crystal nanobeam sensor using optical bistability," in Quantum Electronics and Laser Science Conference (Optical Society of America, 2011).

[10] W. Lai, S. Chakravarty, Y. Zou, Y. Guo, and R. T. Chen, "Slow light enhanced sensitivity of resonance modes in photonic crystal biosensors," Appl. Phys. Lett. 102, 041111 (2013).

[11] L. J. Sherry, S. Chang, G. C. Schatz, and R. P. Van Duyne, "Localized surface plasmon resonance spectroscopy of single silver nanocubes," Nano Lett. 5, 2034–2038 (2005).

[12] Q. Quan, D. L. Floyd, I. B. Burgess, P. B. Deotare, I. W. Frank, S. K. Tang, and M. Loncar, "Single particle detection in CMOS compatible photonic crystal nanobeam cavities," Opt. Express 21, 32225–32233 (2013).

[13] M. Notomi, "Manipulating light with strongly modulated photonic crystals," Rep. Prog. Phys. 73, 096501 (2010).

[14] D. Yang, C. Wang, and Y. Jin, "Silicon On-Chip One-Dimensional Photonic Crystal Nanobeam Bandgap Filter Integrated With Nanobeam Cavity for Accurate Refractive Index Sensing," IEEE Photon. J., vol. 8, no. 2, Apr. 2016, Art. no. 4500608.

[15] Sejeong Kim, "Single nanobeam optical sensor with a high Q factor and high sensitivity", Opt. Lett. 40.005351 (2015)

[16] D. Yang, H. Tian, Y. Ji, and Q. Quan, "Design of simultaneous high-Q and high-sensitivity photonic crystal refractive index sensors," J. Opt. Soc. Am. B 30, 2027–2031 (2013).

[17] D. Yang, S. Kita, F. Liang, C. Wang, H. Tian, Y. Ji, M. Loncar, and Q. Quan, "High sensitivity and high Q-factor nanoslotted parallel quadrabeam photonic crystal cavity for real-time and label-free sensing," Appl. Phys. Lett. 105, 063118 (2014).

[18] D. Yang, H. Tian, and Y. Ji, "High-Q and high-sensitivity width-modulated photonic crystal single nanobeam air-mode cavity for refractive index sensing," Appl. Opt., vol. 54, no. 1, pp. 1–5, Jan. 2015.

[19] A. M. Armani and K. J. Vahala, "Heavy water detection using ultra-high-Q microcavities," Opt. Lett. 31, 1896–1898 (2006).